SAN098-2639C

MATHEMATICAL MODEL OF A LITHIUM/THIONYL CHLORIDE BATTERY

Mukul Jain[a,b], Ganesan Nagasubramanian[c], Rudolph G. Jungst[c] and John W. Weidner[a]

[a] Department of Chemical Engineering
University of South Carolina
Columbia, SC 29208

[b] Present Address: University of New Mexico
Advanced Materials Laboratory
1001 University Blvd., SE • Suite 100
Albuquerque, NM 87106

[c] Lithium Battery Research and Development Department 1521
Sandia National Laboratories
P.O. Box 5800, MS 0613
Albuquerque, NM 87185

ABSTRACT

A one-dimensional mathematical model of a spirally wound lithium/thionyl chloride primary battery has been developed and used for parameter estimation and design studies. The model formulation is based on the fundamental conservation laws using porous electrode theory and concentrated solution theory. The model is used to estimate the diffusion coefficient and the kinetic parameters for the reactions at the anode and the cathode as a function of temperature. These parameters are obtained by fitting the simulated capacity and average cell voltage to experimental data over a wide range of temperatures (-55 to 49°C) and discharge loads (10 to 250 ohms). The experiments were performed on D-sized, cathode-limited, spirally wound lithium/thionyl chloride cells. The model is also used to study the effect of cathode thickness on the cell capacity as a function of temperature, and it was found that the optimum thickness for the cathode-limited design is temperature and load dependent.

INTRODUCTION

The lithium/thionyl chloride battery ($Li/SOCl_2$) has received considerable attention as a primary energy source due to its high energy density, high operating cell voltage, voltage stability over 95% of the discharge, large operating temperature range (-55 °C to 70 °C), long storage life, and low cost of materials [1,2]. However, a loss in performance may occur after periods of prolonged storage at high and low temperatures, or when exposed to intermittent use. This loss in performance may result in reduced capacity or even worse, catastrophic failure especially when operated at high discharge rates. High discharge rates

DISCLAIMER

and high temperatures promote thermal runaway, which can result in the venting of toxic gases and explosion [2].

Mathematical models can be used to tailor a battery design to a specific application, perform accelerated testing, and reduce the amount of experimental data required to yield efficient, yet safe cells. Models can also be used in conjunction with the experimental data for parameter estimation and to obtain insights into the fundamental processes occurring in the battery. Previous investigators have presented one-dimensional mathematical models of the $Li/SOCl_2$ battery. They used porous electrode theory [3] to model the porous cathode, and concentrated solution theory [4] for the electrolyte solution to study the effect of various design and operational parameters on the discharge curves. The theoretical results showed similar qualitative trends to those observed experimentally. However, a lack of experimental data and unknown values for many of the kinetic and transport parameters as a function of temperature prevented quantitative comparisons. Evans and White [5] presented a parameter estimation technique, and used it in conjunction with the one-dimensional mathematical model presented earlier [6]. However, the comparison of the simulated discharge curves with the experimental curves was done only for partial discharge, and at only one ambient temperature. Also, the material balances in these models [6, 7] did not account for the volume differential that arises due to the reduction of $SOCl_2$ to form LiCl. It has been shown [8] that the material balance has to be modified when the reaction in the porous electrode leads to a change in volume in order to predict realistic discharge times.

This paper presents a one-dimensional mathematical model for the $Li/SOCl_2$ cell that includes the volume changes due to the reaction. The model is developed to predict discharge curves at low to moderate discharge rates (discharge loads $\geq$ 10 ohm, corresponding to current densities less than 2 mA/cm^2) where thermal runaway is not a problem. It is used in conjunction with experimental data to obtain estimates for diffusion coefficient and exchange current densities for the reactions at the anode and cathode as a function of temperature. The model shows good agreement with the experimental data over a wide temperature range (-55 to 49 °C). The model is then used to study the effect of cathode thickness on the cell performance as a function of operating temperature.

EXPERIMENTAL

The D-size spirally wound $Li\text{-}SOCl_2$ cells used in the experiments were obtained from Eagle Pitcher Technologies. The cells consisted of a carbon cathode, lithium anode and two Whatman DBS45-1 borosilicate glass separators. The assembly is rolled together (anode, separator, cathode, and then separator), and the roll is inserted into a stainless steel cell can with a pre-welded burst disk in the base. The cell can is equipped with a stainless steel header assembly with pre-welded nickel tabs for the Li anode. The cells were filled in an inert atmosphere of Argon with 28 ml of electrolyte consisting of 1.0 M $LiAlCl_4$ in $SOCl_2$.

The cells were discharged at different loads ranging from 10 ohms to 250 ohms using

an model BT2042 Arbin battery cycler. The discharge measurements were carried out in controlled temperature environment to study the effect of temperature, and the temperature during tests was controlled with a benchtop model Tenney Jr. temperature chamber. A cutoff voltage of 2.0 V was used to note the capacity delivered by the cell for a constant load discharge at a given temperature. Multiple experiments were conducted for the same conditions, and the data reported in this work are an average of three or more experiments.

MODEL DEVELOPMENT

Figure 1 shows a schematic of the one-dimensional cell as modeled in this work. This schematic shows the cross-section of a spirally wound Li/$SOCl_2$ cell. The four regions in the schematic are the lithium foil anode, the lithium chloride (LiCl) film that forms on the anode surface, the separator (usually glass matting), and the porous carbon cathode. The electrolyte consists of 1.5 M lithium tetrachloroaluminate ($LiAlCl_4$) in thionyl chloride ($SOCl_2$). The components are rolled together and inserted in a cylindrical can (commercial D-size). Electrolyte is then poured into the can, filling the porous regions of the roll, and the excess electrolyte resides at the top of the electrode/separator assembly. The anode surface and the cathode current collector are the boundaries of the model region. The overall reactions included in the model are the oxidation of lithium at the anode

$$Li \rightarrow Li^+ + e^- \qquad \text{[reaction 1]}$$

and the reduction of $SOCl_2$ followed by precipitation of LiCl at the cathode

$$4Li^+ + 4e^- + 2SOCl_2 \rightarrow 4LiCl + SO_2 + S \qquad \text{[reaction 2]}$$

The $SOCl_2$ is the solvent, and $LiAlCl_4$ is the electrolyte salt. The following assumptions have been made in this work:

1. LiCl precipitation occurs completely and instantaneously.
2. LiCl film on the anode has constant thickness and porosity.
3. The only species that are accounted for explicitly in the model are $LiAlCl_4$, $SOCl_2$, and LiCl.
4. The temperature is uniform throughout the cell, although it can change with time.
5. The cathode's matrix phase thickness does not vary with time.
6. The electrolyte salt, $LiAlCl_4$, dissociates completely as a binary electrolyte.
7. Partial molar volumes and transference numbers are constant throughout the discharge.
8. Double layer charging in the pores is neglected.
9. Self-discharge is negligible.

Assumption 1 is made due to the low solubility of LiCl in the electrolyte solution ($LiAlCl_4$ in $SOCl_2$) [9]. Although the thickness and porosity of the LiCl film change with storage temperature [10] and mechanical rupture of the film may occur during high-rate discharge [11], the properties of the film do not have a significant effect on the results reported in this work since fresh cells and low discharge rates are used. Assumption 3

holds due to the high solubility of S and SO_2 in the solvent [9], and Cl^- is not included due to instantaneous LiCl formation. The partial molar volume of the solvent was measured with S and SO_2 present in solution [12], so the volume they occupy is implicitly accounted for in the model. Assumption 4 is valid for low-to-moderate rate cells where thermal runaway is not a major concern [6]. The cathode thickness is assumed to be constant during the discharge (assumption 5), although the changes in the dimension due to cathode swelling are incorporated in the initial thickness and porosity of the cathode matrix phase, as explained later in this work. The partial molar volume of the solvent does not vary much with temperature and salt concentration [13] (assumption 7), and neglecting the double layer charge should be valid at the current densities used in this work (assumption 8). The biggest possible role of self-discharge in the performance of these cells during constant load discharge would be to render them anode limited. In all experimental data used in this work, some of the lithium anode remained after complete discharge. Therefore, assumption 9 is valid.

Conservation of mass and current, species transport, and reaction kinetics are used to formulate the governing equations for the $Li/SOCl_2$ cell. Macroscopic theory of porous electrodes [3, 4] is employed, where the porous region is considered to be a superposition of two continua, the electrolyte (ionically conducting solution phase) and the matrix (electronically conducting solid phase). The dependent variables are averaged over a differential volume of this two-phase continuum. These averaged quantities are continuous in time and space, and the differential volume element is large compared to the pore dimensions, yet small relative to the electrode dimensions. The model development is similar to the one presented earlier [5, 7] except for the material balance correction related to the volume reduction [8], and therefore the equations are not presented in this work. The precipitation of LiCl in the porous cathode also results in an expansion of the cathode, known as cathode swelling. The effect of cathode swelling on the dimensions of the cathode will be treated here by modifying the cathode's matrix-phase thickness and porosity, as explained later in the parameter estimation section.

Method of Solution

The system of coupled, nonlinear, partial differential equations describing the $Li/SOCl_2$ cell is solved numerically. The spatial derivatives are approximated using three point finite differences, and implicit stepping is used for the time derivatives. The resulting set of coupled, nonlinear, algebraic equations is solved using deBoor's banded matrix solver [14], which employs a Newton-Raphson algorithm. The procedure is iterative and requires initial guesses of the unknowns, which were the converged values of the previous time steps.

RESULTS AND DISCUSSION

Some of the parameters are either available in the literature (*e.g.*, conductivity) or known at the time of cell assembly (*e.g.*, cathode thickness). Although the literature contains conductivity data, it is not available over the entire range of temperature needed

nor is it in a form convenient to be used in the model. Therefore, correlations were developed for conductivity as a function of concentration and temperature using the data available in literature [15, 16]. The other parameters given in Table I are either not available (*e.g.*, transport and kinetic parameters), change during discharge (*e.g.*, cathode thickness due to swelling), or depend on how the data is collected (*e.g.*, external heat transfer coefficient). Therefore, the first task was to use the model to estimate all unknown parameters. A sequential approach to the requisite parameter estimation is described below. Although this approach may seem simplistic, it resulted in parameter values that make physical sense and enable the model to predict the cell behavior over a wide range of operating conditions. The validity of the estimated parameters and the interactions among them is validated later by simulating the entire discharge curves and comparing them with the experimental discharge curves over the entire operating range of temperature and load.

External Heat Transfer

The heat transfer coefficient was obtained by matching the simulated temperature rise in the cell to the rise in skin temperature observed experimentally. At most temperatures and loads, the temperature rise was small. However, at 25°C and 10 Ω (*i.e.*, a high current), the skin temperature rose by approximately 5 °C. Under these operation conditions, the heat-transfer coefficient was adjusted in the model until a temperature rise of 5 °C was obtained. The value of the heat-transfer coefficient, $h_o = 6\times10^{-4}$ J/cm^{2}K, was used for all subsequent simulations. This value is consistent with that used in earlier models [6].

Cathode Dimension (Effect of Swelling)

The thickness and porosity of the porous cathode are measured prior to assembly. Due to excess electrolyte in the header of the cell, the battery will continue to discharge until the front of the porous cathode becomes plugged with LiCl. Therefore, the maximum capacity of the cell can be calculated based on the volume available for LiCl precipitation. If we use the porosity and thickness values prior to assembly, the maximum capacity is much lesser than observed experimentally. The extra capacity can be attributed to the increased volume due to cathode swelling.

The extent of cathode swelling can be estimated by assuming the highest capacity obtained experimentally (16.2 Ah at 250 ohms and 25 °C) represents about 97% of the theoretical capacity, or Q_{max} = 16.7 Ah. A discharge efficiency of 97% was arrived at by noting that when diffusion and kinetic contributions to the non-uniformity are minimized (*i.e.*, large diffusion coefficient and small exchange current density for $SOCl_2$ reduction), ohmic losses lead to a capacity loss of about 2%. Assuming an additional 1% loss due to diffusion and kinetic effects leads to a total efficiency of 97%. Using this information along with the initial dimensions of the electrode, and noting that the increase in available volume for LiCl precipitation is solely due to increased porous region since no matrix phase is added, the initial porosity and thickness of the cathode is modified.

Diffusion Coefficient

There is no data available in the literature on the diffusion coefficient of $LiAlCl_4$ in $SOCl_2$. However, the model can be used to obtain the diffusion coefficient, D, as a function of temperature by recognizing that kinetic and mass transfer resistances increase as the temperature decreases. Since a large kinetic resistance leads to uniform reaction and a large mass-transfer resistance has the opposite effect, premature plugging of the pores at the front of the electrode at low temperatures is dominated by mass-transfer limitations. As will be verified later, the simulated capacity was not affected by the $SOCl_2$ kinetics for all loads at –55, -40 and –18 °C, and the 10 Ω load at 25 °C. Therefore, capacity data at low temperatures can be used to get the diffusion coefficient, D, as a function of temperature and the transference number, t_+°. The transference number was adjusted such that D is relatively insensitive to the loads and t_+° is insensitive to temperature. A value of $t_+^\circ = 0.7$ met this criteria. The estimated diffusion coefficients at different temperatures were used to obtain the following relation

$$D = 1.726\times10^{16}\exp\left(-\frac{2.315\times10^{4}}{T}+\frac{2.395\times10^{6}}{T^{2}}\right)$$

where T is in K. Equation [44] fits the data well except at -40 °C. At this temperature the value of D that enables the model to accurately predict the capacity is a function of load.

Kinetics for the Main Reaction at the Cathode

In contrast to lower temperatures, the discharge capacity at high temperatures is dictated by the kinetics for $SOCl_2$. Facile kinetics yields a non-uniform reaction in porous electrodes [4], which results in premature pore plugging at the front of the electrode. Therefore, the capacity data for all loads at 25 and 49 °C was used to estimate the kinetic parameters for $SOCl_2$ reduction, $i_{o,2,ref}$ and $\alpha_{c,2}$ (it is assumed that $\alpha_{a,2} + \alpha_{c,2} = 2$). As with the diffusion coefficient, $i_{o,2,ref}$ was obtained by fitting the simulated capacity to the experimental capacity. The cathodic transfer coefficient, $\alpha_{c,2}$ was adjusted such that it was insensitive to load and temperature, and $i_{o,2,ref}$ was insensitive to the load. The result is $\alpha_{c,2} = 0.3$, and a value for $i_{o,2,ref}$ at the two temperatures. The $i_{o,2,ref}$ values at these two temperatures was fit to an Arrhenius expression to give

$$i_{o,2,ref} = 2.5\times10^{3}\exp\left(-\frac{5500}{T}\right)$$

where T is in K.

Kinetics for the Main Reaction at the Anode

Once the $SOCl_2$ reduction kinetics and the electrolyte diffusion coefficient are known, the only unknown is Li oxidation kinetics. Li oxidation does not affect the cell capacity [6], but it may affect on the cell voltage. The difference in the cell potential and the open-circuit potential is due to the kinetic loss at the anode, ohmic loss in the separator and kinetic loss in the porous cathode. The losses through the separator and the porous

cathode were calculated using the known conductivity and $SOCl_2$ reduction kinetic parameters. These two losses accounted for the entire voltage loss at high temperature and high load (*i.e.*, low current). Therefore, the loss due to Li oxidation at the anode was negligible except at low temperature and low loads. Using the calculated overpotential at –18, -40, and –55 °C for loads of 10 and 50 ohms, a transfer coefficient, α_a, of 0.8 was obtained that made the exchange current density insensitive to the load at low temperatures. Equation [25] was used to obtain the exchange current density for Li oxidation, $i_{o,1,ref}$ and the temperature dependence of $i_{o,1,ref}$ is given as

$$i_{o,1,ref} = 1.157 \times 10^3 \exp\left(-\frac{4641}{T}\right)$$

where T is in K.

Comparison of Experimental data and Model Simulations

Although the parameters are obtained sequentially, the interactions between the various phenomena such as mass-transfer and kinetics have to be captured in order to predict the cell performance with accuracy. The validity of these interactions and the estimated parameters can be confirmed by simulating the entire discharge curves and comparing them to the experimental discharge curves. Figure 2 shows the comparison of the simulated discharge curves with the experimental discharge data obtained at -55, -18 and 25 °C for 50 ohms load. Figure 3 shows the comparison at –18°C for loads of 10, 50 and 250 ohms. Overall a very good agreement is observed between the experimental and simulated discharge curves over the entire range of temperature and loads.

The validity of the estimated parameters over the entire range of temperature and load can be shown by summarizing the match of simulated results with experimental data. Figures 4 and 5 compare the capacity and average cell voltage, respectively, for the experimental and simulated discharge curves. Again, the symbols represent the experimental values, and are a mean of at least three experimental data, while the error bars represent the range of the data. The cutoff voltage used for the capacity shown in Figure 4 was 2.0 V for both the experimental and simulated data. The low capacity at lower temperatures is due to mass transfer limitations in the cathode, while the slight drop in capacity at higher temperatures and lower loads (higher currents) is due to the non-uniform reaction caused by facile kinetics in the cathode. Good agreement between simulated and experimental capacity over the entire range of temperature and load is obtained, with a major exception at –40 °C. As mentioned earlier, no single value of D could be estimated that would fit the experimental capacity at –40 °C for both the loads (50 and 250 ohms). Capacity data for more loads at –40 °C might be useful in providing more confidence in the estimated diffusion coefficient.

The comparison of the experimental and simulated cell voltage shown in Figure 5 are for the cell voltage at half the capacity delivered. The capacity that was delivered at a cutoff voltage of 2.0 V was noted, and the simulated and experimental cell voltage at half of that capacity were compared. As evident from the figure, the simulated cell voltage fits the experimental values fairly well over the entire range of temperature and load.

Cathode Thickness Optimization

With a reliable set of parameters, the model can be used to perform design studies. For example, Figure 6 shows the effect of cathode thickness on the cell capacity for various temperatures for a constant load of 50 ohms. For the results shown in Figure 6, the following three parameters were held constant at the value of the experimental cells: (*i*) the ratio of the anode capacity to cathode capacity; (*ii*) the ratio of anode area to the cathode; and (*iii*) the separator thickness. The solid lines show the predicted capacities from the model and the dashed line is the theoretical capacity for a given thickness. The theoretical capacity is obtained when all the pores in the cathode are uniformly filled with LiCl precipitate for a cathode limited design (*i.e.*, the capacity in the anode (Li foil) is more than the cathode). The separators constitute most of the cell volume for thin cathodes, and so the theoretical cell capacity is low. As the cathode thickness increases, the theoretical capacity increases because the separator accounts for proportionately less of the cell volume. The theoretical capacity of the cell eventually levels off as cathode active material becomes essentially all cell volume.

In Figure 6, the ohmic, kinetic or mass-transfer limitations do not arise in the thin cathodes at high temperatures, and this leads to capacities close to theoretical maximum. However, ohmic and mass-transfer limitations at lower temperatures lead to lower than theoretical capacities. As the cathode's thickness increases, it's area decreases since the total volume is conserved. This results in an increase in current density for the same load, and therefore a less uniform reaction. The mass-transfer limitations are insignificant at higher temperatures, but the facile kinetics lead to non-uniformity in the reaction in the porous electrode. For example, at cathode thickness greater than 1 mm, the reaction is more non-uniform at 49 °C compared to 25 °C, resulting in lower capacity. There exists an optimum thickness at a given load and temperature when the cell capacity is a maximum. For the D-size cell shown here, a cathode thickness of approximately 0.15 cm at 25 °C and 50 ohm load would result in maximum capacity.

CONCLUSIONS

A one-dimensional mathematical model for the lithium/thionyl chloride primary battery has been developed and used for parameter estimation and design studies. The model formulation is based on the fundamental conservation laws using porous electrode theory and concentrated solution theory. The material balance in the model has been modified to account for the volume reduction that occurs in the porous cathode on discharge. The model was used to estimate the diffusion coefficient, and the kinetic parameters for the reactions at the anode and the cathode as a function of temperature. These parameters were obtained by fitting the simulated capacity and average cell voltage to the experimental capacity and average cell voltage, respectively, over a wide range of temperatures (-55 to 49°C) and discharge loads (10 to 250 ohms). The experiments were performed on D-sized, cathode-limited, spirally-wound lithium/thionyl chloride cells. It was found that the cell capacity was governed by the material transport at lower temperatures, while the $SOCl_2$ reduction kinetics controlled the capacity at higher

temperatures (25 °C and above). The model was then used to study the effect of cathode thickness on the cell capacity as a function of temperature. An optimum thickness exists depending on the temperature in order to deliver maximum capacity.

ACKNOWLEDGEMENTS

The authors acknowledge the financial support of Sandia National Laboratories. Sandia is a multiprogram laboratory operated by Sandia Corporation, a Lockheed Martin Company, for the United States Department of Energy under contract No. DE-AC04-94AL85000. Experimental measurements of cell capacity and voltage were conducted by H. L. Case at Sandia National Laboratories.

REFERENCES

1. D. H. Johnson, A. D. Ayers, R. L. Zupancic, V. S. Alberto, and J. C. Bailey, *J. Power Sources*, **2**, 61 (1984).
2. S. Surampandi, G. Halpert, and I. Stien, JPL Publication 86-15, (June 1986).
3. J. Newman and W. Tiedemann, *AIChE. J.*, **21**, 25 (1975).
4. J. Newman, "Electrochemical Systems", Prentice Hall, Inc., Englewood Cliffs, New Jersey (1973).
5. T. I. Evans and R. E. White, *J. Electrochem. Soc.*, **136**, 2798 (1989).
6. T. I. Evans, T. V. Nguyen, and R. E. White, *J. Electrochem. Soc.*, **136**, 328 (1986).
7. K. Tsaur and R. Pollard, *J. Electrochem. Soc.*, **131**, 975 (1984).
8. M. Jain and J. W. Weidner, submitted to *J. Electrochem. Soc.*, July 1998.
9. J. R. Driscoll, G. L. Holleck, and D. E. Toland, in "Proceedings of the 27th Power Sources Symposium," Atlantic City, NJ, June 21-24, 1976.
10. A. N. Dey, *Thin Solid Films*, **43**, 131 (1977).
11. A. N. Dey, *Electrochim. Acta*, **21**, 377 (1976).
12. S. Szpak and H. V. Venkatasetty, *J. Electrochem. Soc.*, **131**, 961 (1984).
13. J. S. Dunning, D. N. Bennion, and J. Newman, *J. Electrochem. Soc.*, **120**, 906 (1973).
14. C. DeBoor, "A practical Guide to Splines," Springer-Verlag New York Inc., New York (1978).
15. H. V. Venkatasetty and D. J. Saathoff, *J. Electrochem. Soc.*, **128**, 773 (1981).
16. R. W. Berg, H. A. Hjuler, A. P. L. Sondergaard, and N. J. Bjerrum, *J. Electrochem. Soc.*, **136**, 323 (1989).

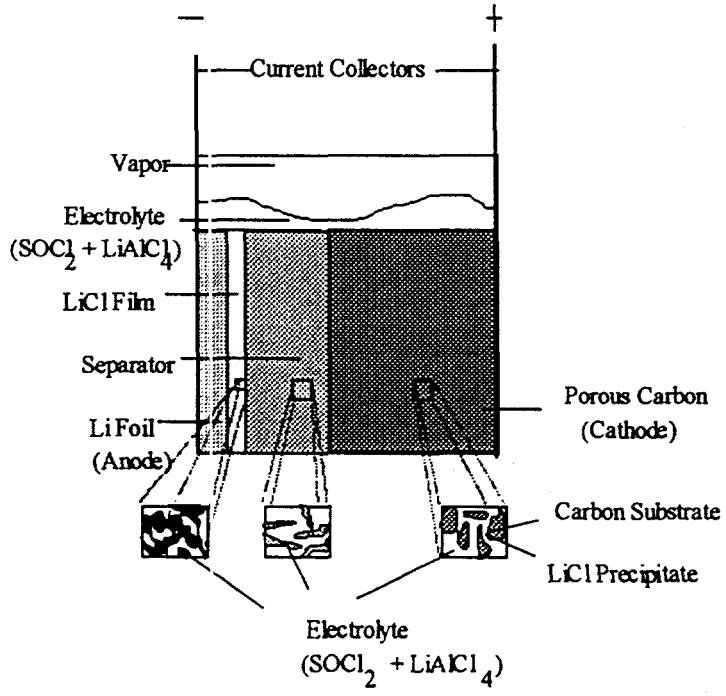

Figure 1. Schematic of a lithium/thionyl chloride cell. The anode, separator and the porous cathode are stacked together, and the assembly is spirally wound and inserted in a D size cell.

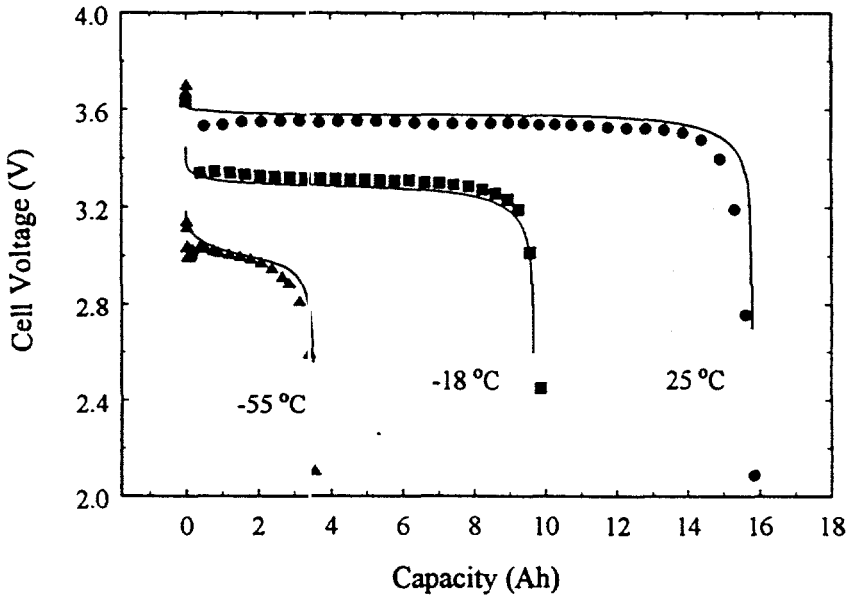

Figure 2. Comparison of experimental and simulated discharge curve for a 50 ohm load at -55, -18 and 25 °C. The symbols represent the experimental data while the solid line is for the model simulation.

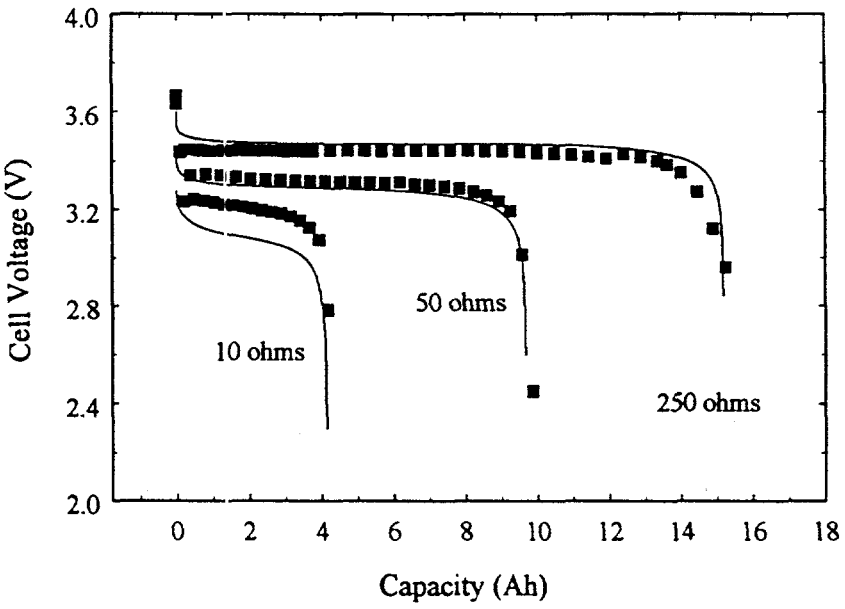

Figure 3. Comparison of experimental and simulated discharge curves for loads of 10, 50 and 250 ohms at −18 °C. The symbols represent the experimental data while the solid line is for the model simulation.

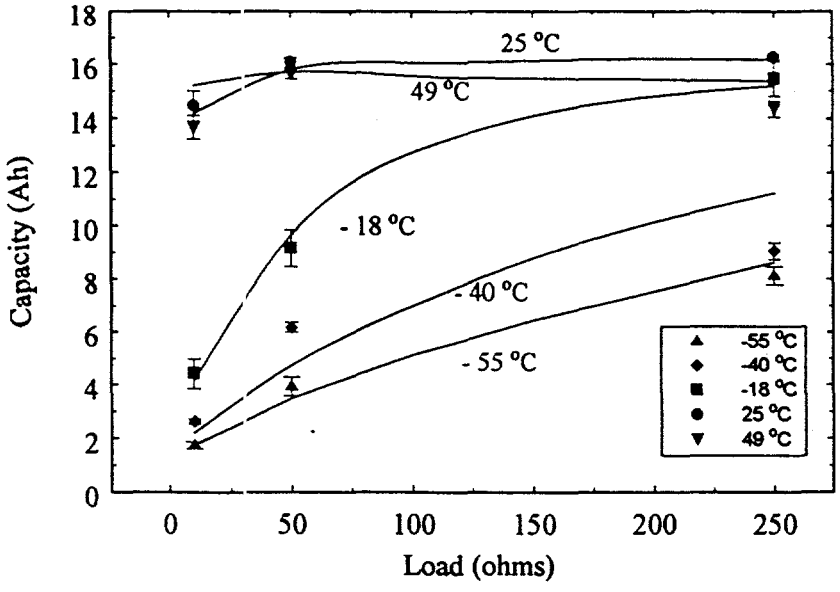

Figure 4. Comparison of the simulated and experimental utilization as a function of the load, over a temperature range. The solid lines represent the simulated cell voltage and the symbols are the experimental data.

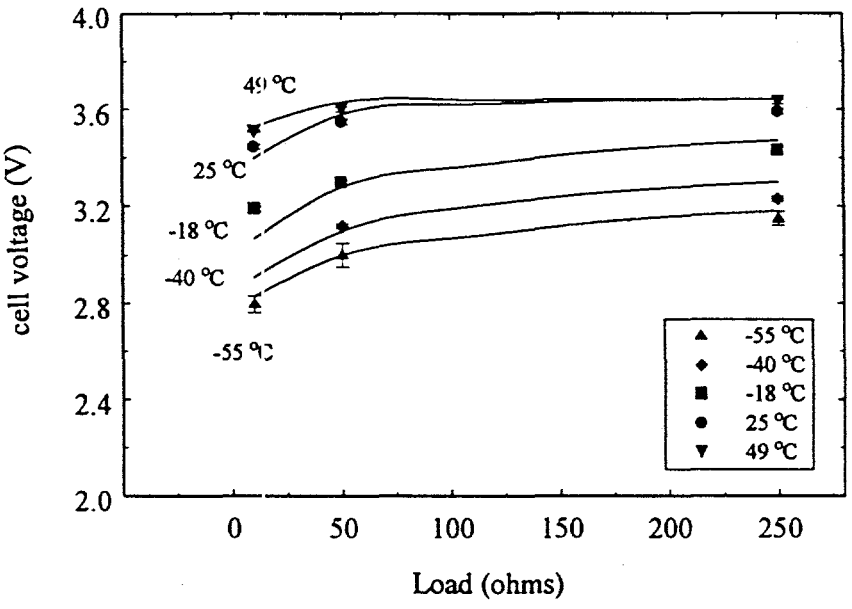

Figure 5. Comparison of the simulated and experimental cell voltage (at half the capacity as a function of the discharge loads over a temperature range (-55 to 49 °C). The solid lines represent the simulated cell voltage and the symbols are the experimental data.

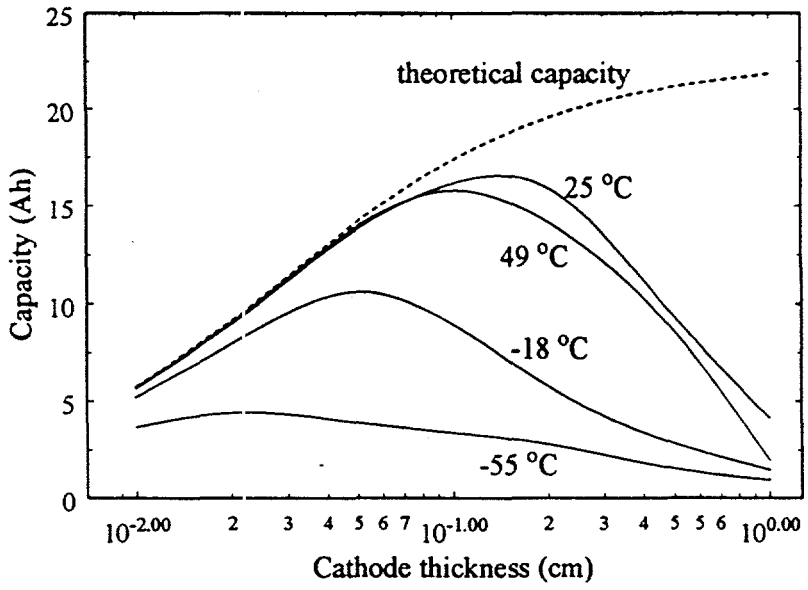

Figure 6. Effect of cathode thickness on the cell capacity for various temperatures at a constant load of 50 ohms. The theoretical capacity (-----) is also shown for a D-size cell as a function of the cathode thickness.